Observations of Double Layers in Earth's Plasma Sheet

R. E. Ergun,[1,2] L. Andersson,[2] J. Tao,[1,2] V. Angelopoulos,[3] J. Bonnell,[4] J. P. McFadden,[4] D. E. Larson,[4] S. Eriksson,[2] T. Johansson,[2] C. M. Cully,[5] D. N. Newman,[6] M. V. Goldman,[6] A. Roux,[7] O. LeContel,[7] K.-H. Glassmeier,[8] and W. Baumjohann[9]

[1]*Department of Astrophysical and Planetary Sciences, University of Colorado, Boulder, Colorado 80309, USA*
[2]*Laboratory for Atmospheric and Space Physics, University of Colorado, Boulder, Colorado 80309, USA*
[3]*Institute of Geophysics and Planetary Physics, University of California, Los Angeles, California 90055, USA*
[4]*Space Sciences Laboratory, University of California, Berkeley, California, 94720, USA*
[5]*Swedish Institute of Space Physics, Uppsala, Sweden*
[6]*Center for Integrated Plasma Studies, University of Colorado, Boulder, Colorado 80309, USA*
[7]*Centre d'étude des Environnements Terrestre et Planétaires, Velizy, France*
[8]*TUBS, Braunschweig, D-38106, Germany*
[9]*Space Research Institute, Austrian Academy of Sciences, A-8042 Graz, Austria*
(Received 22 January 2009; published 16 April 2009)

We report the first direct observations of parallel electric fields ($E_\parallel$) carried by double layers (DLs) in the plasma sheet of Earth's magnetosphere. The DL observations, made by the THEMIS spacecraft, have $E_\parallel$ signals that are analogous to those reported in the auroral region. DLs are observed during bursty bulk flow events, in the current sheet, and in plasma sheet boundary layer, all during periods of strong magnetic fluctuations. These observations imply that DLs are a universal process and that strongly nonlinear and kinetic behavior is intrinsic to Earth's plasma sheet.

DOI: 10.1103/PhysRevLett.102.155002 PACS numbers: 94.30.ct, 52.35.Mw, 94.05.Pt, 94.30.cp

The discussion of parallel electric fields ($E_\parallel$) in cosmic plasmas began decades ago [1], focusing on whether they exist in collisionless plasmas and, if so, their possible impact. Parallel electric fields not only break the frozen-in condition, a critical axiom of ideal magnetohydrodynamics, but they accelerate electrons and ions creating a highly unstable and turbulent plasma environment. The development of double layer (DL) theory [2] and subsequent verification in laboratory experiments [3] demonstrated that $E_\parallel$ could be carried by self-consistent, Debye-scale structures.

Parallel electric fields are understood to accelerate electrons and ions in the auroral regions [4]. Auroral satellites have provided direct observation of DLs [5–7] whose properties are understood through analysis and simulation [2,8–13]. The auroral $E_\parallel$ structures are primarily associated with global field-aligned current systems and strong Alfvén wave-driven currents.

The auroral observations prove that DLs naturally occur, but are limited to a region known to have highly kinetic, nonideal processes. Here, we report direct observations of DLs well outside of the auroral acceleration region, in Earth's plasma sheet (PS). These DLs are observed during periods of strong magnetic fluctuations in several distinct regions of the PS including the boundary layer, the current sheet, and in association with rapid earthward flows known as bursty bulk flows [14,15]. This widespread observation of DLs not only suggests that parallel electric fields are universal in collisionless plasmas but that many active plasma regions, including astrophysical plasmas, may be subject to strongly nonlinear and nonideal behavior.

The observations are from the THEMIS mission [16] which has five identical satellites, designated probes *A*–*E*, in highly eccentric orbits at low inclination with apogees of $\sim 10 R_E$ (probe *A*), $\sim 12 R_E$ (probes *E* and *D*), $\sim 20 R_E$ (probe *C*), and $\sim 30 R_E$ (probe *B*). The orbital periods are integer multiples of each other causing the satellites periodically to "line up" in the PS so that the timing of magnetic substorms can be understood. The satellites carry electron and ion analyzers [17], a three-axis electric field instrument (dc—8 kHz) [18,19], and ac and dc [20] magnetometers.

Figure 1 displays a 10-min period of enhanced magnetic fluctuations observed by THEMIS *D* in the PS $\sim 10 R_E$ from Earth's center. Figure 1(a) plots the electron differential energy flux as a function of energy (vertical axis) and time (horizontal axis). The energy flux is calculated from a set of two-dimensional energy-angle measurements averaged over a satellite spin period ($\sim$3 s) [17]. Data from two detectors are combined into a single plot. The low-energy electrons ($\sim$10 eV– $\sim$ 30 keV) are detected by an electrostatic analyzer whereas the higher-energy electrons are detected by a solid state telescope. These data indicate the presence of $\sim$200 eV– $\sim$ 10 keV electrons that are typical of the PS. The lowest-energy electron fluxes are spacecraft photoelectrons. The overlying black trace [Fig. 1(a)] is the electron temperature (T_e) in electron volts derived from the electrostatic analyzer.

Figure 1(b) plots the differential energy flux of ions in the same format. A small gap in energy coverage is seen in the plot as white space. The plot shows high ion fluxes at several kilovolts which also are typical of the PS.

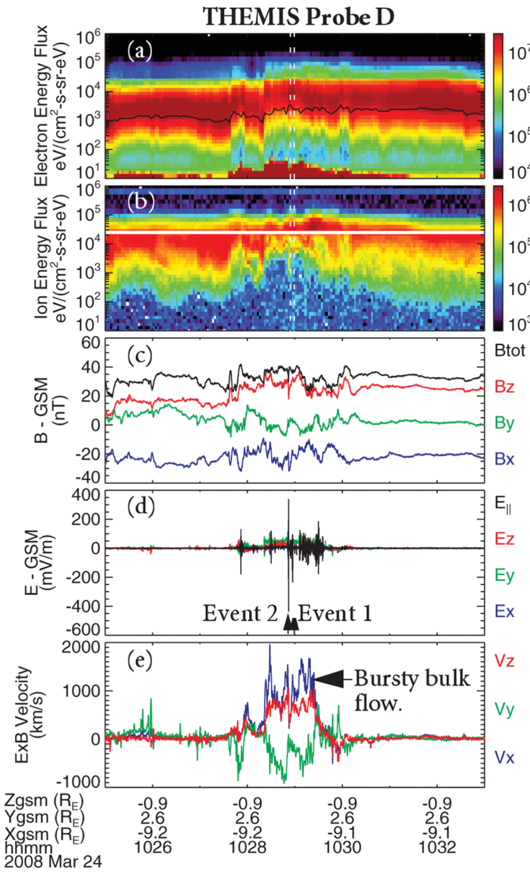

FIG. 1 (color). (a) Electron differential energy flux as a function of energy (vertical axis) and time (horizontal axis). (b) Ion differential energy flux. (c) Magnetic field in GSM [17] coordinates at 128 samples/s. The black trace is $|\boldsymbol{B}|$. (d) The electric field in GSM coordinates at 128 samples/s. The black trace is $E_\parallel$. (e) $\boldsymbol{E} \times \boldsymbol{B}/\boldsymbol{B}^2$ low-pass filtered to 1 Hz. The vertical dashed lines mark two of the DL events.

Figures 1(c) and 1(d) plot the magnetic field ($\boldsymbol{B}$) and the electric field ($\boldsymbol{E}$) in the geocentric solar magnetospheric (GSM) [21] coordinate system: blue is towards the sun, red is near Earth's magnetic north, and green completes the set. The black trace in Fig. 1(c) is $|\boldsymbol{B}|$. $\boldsymbol{B}$ is measured to an accuracy <1 nT [20]. $\boldsymbol{E}$ is measured by three orthogonal dipole antennas [18]. The black trace in Fig. 1(d) represents $E_\parallel$. The antennas in the spin plane of the spacecraft, mostly the GSM x and y directions, have ~40 and ~50 m physical lengths and are accurate to approximately ±2 mV/m depending on plasma conditions. The spin-axis dipole, mainly the GSM z direction, is a ~7 m dipole and is accurate to ±20 mV/m. In Fig. 1, $\boldsymbol{E}$ and $\boldsymbol{B}$ are at 128 samples/s after low-pass filtering to 50 Hz.

Figure 1(e) plots the quantity $\boldsymbol{E} \times \boldsymbol{B}/\boldsymbol{B}^2$ low-pass filtered to 1 Hz. The flow perpendicular to $\boldsymbol{B}$ in the x direction (towards Earth; blue trace) rises to over 1000 km/s from ~10:28 UT to ~10:30 UT, indicating a bursty bulk flow event [14,15]. Such events are associated with magnetic reconnection occurring antiearthward of the spacecraft's position. During the bursty bulk flow event, the electron and ion energies increase [Figs. 1(a) and 1(b)] and $\boldsymbol{E}$ and $\boldsymbol{B}$ display strong variations [Figs. 1(c) and 1(d)].

At the time marked "Event 1" in Fig. 1(d), $\boldsymbol{E}$ was available at higher time resolution, 8192 samples/s (filtered to ≤ 3.3 kHz). Figures 2(a)–2(c) display $E_\parallel$ and two components of the perpendicular electric field: $E_{\rm SP}$ is the component measured only by the spin-plane booms and $E_{\rm perp}$ completes the vector. $E_\parallel$ displays strong turbulence in the form of electron phase-space holes (bipolar structures from −0.05 to 0.10 s) and a unipolar electric field from 0.12 to 0.14 s. This signature, a unipolar $E_\parallel$ structure adjacent to a turbulent region of electron phase-space holes, is identical to that of DLs observed in the auroral ionosphere [5,6] and shown in Figs. 2(e) and 2(f). The auroral DL is verified by an electron beam [Fig. 2(e)] consistent with the DL potential. It also is reproduced by open-boundary Vlasov simulations [11] displayed in Fig. 2(g). The simulation shows a relatively smooth "ramp" region (corresponding to the unipolar $E_\parallel$ structure) adjacent to a series of electron phase-space holes. The THEMIS observations in the PS display these same characteristics.

The speed (v_E) along $\boldsymbol{B}$ of the $E_\parallel$ structure [in Fig. 2(a)] is needed to estimate its physical size and net potential. There is no detectable time delay between individual antenna signals (< ~0.1 ms over a ~25 m baseline), so we conclude that $v_E > 250$ km/s. DLs in the aurora are observed to travel along $\boldsymbol{B}$ roughly at the ion acoustic speed (v_s). This speed is theoretically predicted [10] and verified by simulations [11]. The dominant ion in the PS is H^+ and, at the time of the observation, $T_e \sim 3$ keV and the ion temperature (T_i) is ~20 keV implying that $v_s \sim 1400$ km/s. It is reasonable to conclude that $\sim 250 < v_E < \sim 1400$ km/s.

Given the estimated speeds and the measured time duration (~0.02 s), the parallel size of the $E_\parallel$ structure ($L_\parallel$) ranges from $\sim 5\lambda_D$ to $\sim 30\lambda_D$, where λ_D is the electron Debye length ($\lambda_D \sim 1$ km; the plasma density is $\sim 0.2\ \text{cm}^{-3}$). The potential of the $E_\parallel$ structure [$\Phi_{\rm DL} = \int (E_\parallel v_E) dt$] is between ~250 and ~1400 V. Given the $E_\parallel$ signal characteristics (a unipolar ramp adjacent to a turbulent region), the estimated size of the structure, and the estimated potential, we conclude that the $E_\parallel$ structure is consistent with the DL description.

The $E_\parallel$ structure marked "Event 2" in Fig. 1 has an unusually large amplitude (~250 mV/m). The highest resolution data are not available so $E_\parallel$ is plotted at 128 samples/s in Fig. 2(d). This sample rate is insufficient to resolve electron phase-space holes (typically ~1 ms), but can resolve the $E_\parallel$ structure (~50 ms). As in the case above, $250 < v_E < 1400$ km/s, so again $L_\parallel \sim 5\lambda_D$ to $30\lambda_D$, but $\Phi_{\rm DL}$ is between ~1.5 and ~14 kV. The potential of this event could exceed T_e, ~3 keV.

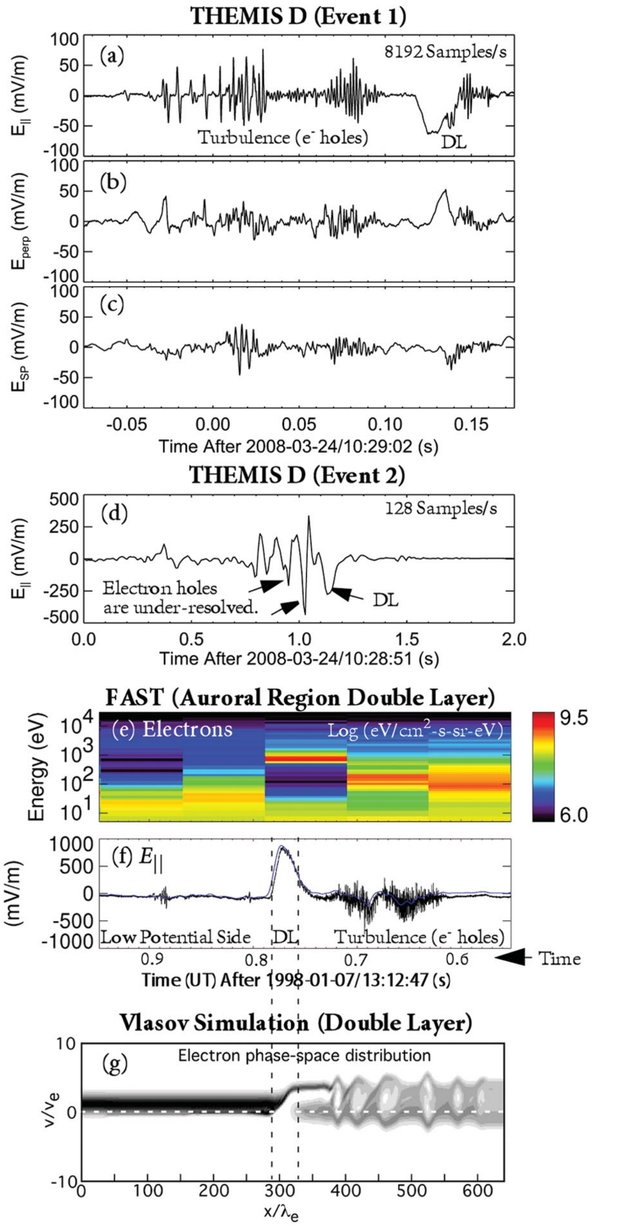

FIG. 2 (color). (a) $E_{\parallel}$ at 8192 samples/s during the period marked "Event 1" on Fig. 1. (b),(c) $E_{\perp}$. The component labeled E_{SP} is from the long wire antennas and accurate to ± 2 mV/m. (d) $E_{\parallel}$ at 128 samples/s during the period marked "Event 2" on Fig. 1. (e),(f) (Derived from [6]) Electron energy flux and $E_{\parallel}$ of an auroral DL at 32 768 samples/s. The DL is bounded by dashed lines. (g) (Derived from [11]) A snapshot in time of phase space of a DL. The vertical axis is velocity and the horizontal axis is distance along $\boldsymbol{B}$.

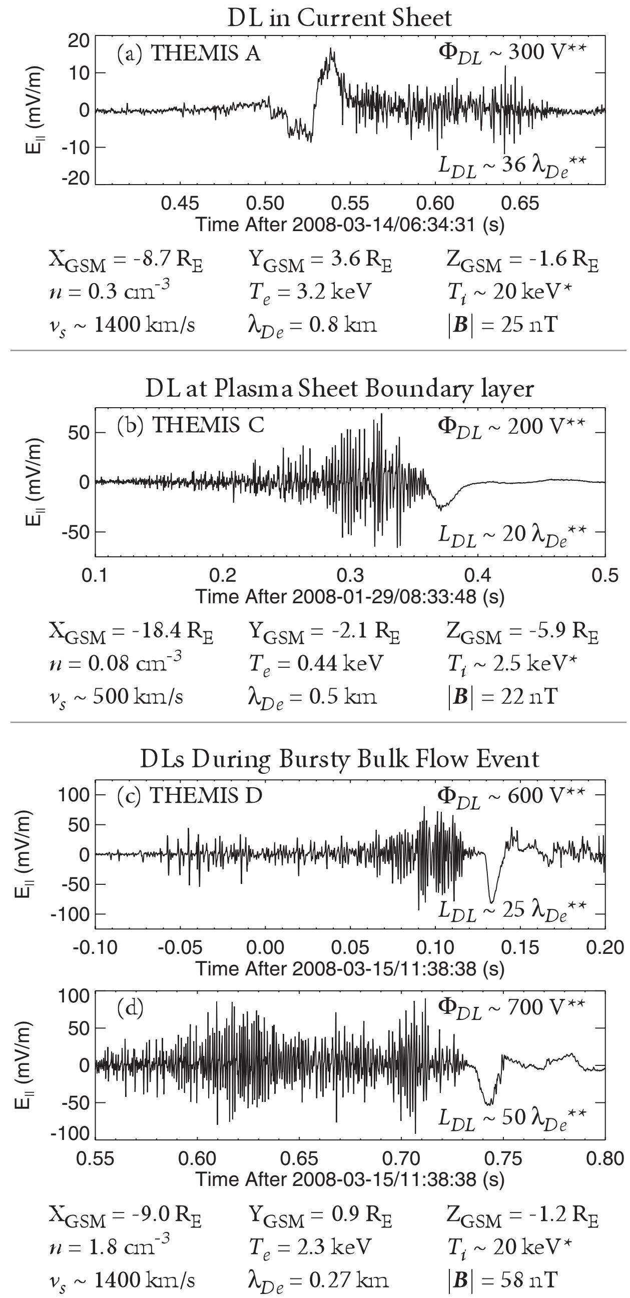

FIG. 3. (a)–(d) $E_{\parallel}$ at 8192 samples/s. The plasma conditions are below. The values marked (*) are estimates. The values marked (**) are calculated assuming that the DL is moving as v_s.

Figure 3 displays the $E_{\parallel}$ signal of four more DLs in the PS observed by the THEMIS satellites at high time resolution (8192 samples/s). All have the same characteristic signature: a nearly unipolar $E_{\parallel}$ structure adjacent to a turbulent region of electron phase-space holes. The polarity of the electron phase-space holes (negative then positive or positive then negative) is consistent with the high-potential side of the DL (electron acceleration). All are observed during periods of strong fluctuations in $\boldsymbol{B}$ and $\boldsymbol{E}$. Assuming that the DLs travel at the ion acoustic speed, all are on the order of $10\lambda_D$ with potentials comparable to T_e. The DLs are observed primarily in three plasma environments: (1) at the plasma sheet boundary layer, (2) near the current sheet where $|\boldsymbol{B}|$ is minimum, or (3) during bursty bulk flows events.

The event in Fig. 3(a) is in the PS $\sim 10R_E$ from Earth's center. Properties of the DL, the location, and plasma conditions are below the plot. It is associated with Alfvénic activity during a dipolarization event ($|B_z|$ increases while $|B_x|$ decreases). Nearby spacecraft, THEMIS *D* and *E*, observed a similar magnetic signature (dipolarization) and an auroral brightening was seen by an all-sky camera of the THEMIS ground network [16]. The DL has a peak amplitude of 20 mV/m, endures for $\sim$25 ms, and could have a speed up to $v_s \sim 1400$ km/s, so the net potential is up to several hundred volts. Since $T_e \sim 3$ keV during the event, the DL would be classified as "weak."

The event in Fig. 3(b) was observed by THEMIS *C* at the plasma sheet boundary layer $\sim 19R_E$ from Earth's center. Two other DLs (not shown) appear within 45 s. This boundary region is between cold plasma ($T_e < 10$ eV) in the magnetotail lobes and hot plasma in the PS ($T_e >$ 100 eV). Figures 3(c) and 3(d) display two additional DLs during a bursty bulk flow event at $\sim 10R_E$. These events display the characteristic signal of a DL [5,6]. Both display low-frequency turbulence on the low-potential (right) side indicating that the accelerated ions may be unstable.

The detection of the tens of DLs in the PS has several far-reaching implications. DL observations should be statistically very rare since they occupy a very small spatial volume. In addition, THEMIS burst data (highest resolution) are available for less that 0.05% of the orbit, albeit the events are selected on electric field amplitude by an on-board algorithm. It appears that DLs may be a frequently occurring phenomenon in the PS during magnetic activity.

A simple estimate of the influence of DLs can be made by assuming that the on-board algorithm is 100% efficient in selecting DLs. The transverse (to $\boldsymbol{B}$) scale ($L_\perp$) of DLs ranges from tens of λ_D (1 km) to perhaps an ion scale size, $\delta_i = c/\omega_{pi}$ (300 km). Since they travel at v_s ($\sim$1000 km/s) along $\boldsymbol{B}$, the physical size ($L_\parallel \sim 10\lambda_D$) is not germane; rather, one considers the rate of volume that they transit, $\dot{V} \sim 10^8$ km^3/s if $L_\perp \sim \delta_i$. The PS covered by THEMIS, that from 10–30R_E, 30R_E wide and 10R_E thick, is roughly 3×10^{15} km^3. In a three-month period, the THEMIS satellites spend <50% of the time in the PS and, during that period (4×10^6 s), the magnetotail was strongly magnetically active roughly $\sim$2% of the time yielding 1×10^5 s of coverage by each of five satellites. Given tens of DL observations (as of this publication), one can infer that thousands of DLs (if $L_\perp \sim \delta_i$) are in the near-Earth PS at all times during magnetically active periods ($>10^6$ DLs if $L_\perp \sim 1\lambda_D$).

Given the above analysis, DLs cover $\sim 10^8$ km^2 of magnetic flux tube area (if restricted to one DL per flux tube; this estimate is independent of $L_\perp$) out of a total of PS cross section of 10^{10} km^2. At active times, 1% or more of the PS flux tubes are undergoing nonideal behavior including electron and ion acceleration.

The DLs appear to have several different origins. Those observed outside of $\sim 15R_E$ are related to either the PS-lobe boundary or activity generated by magnetic reconnection. The DL formation in the PS-lobe boundary may result from currents driven through a strong temperature gradient since the PS-lobe boundary can have a mixture of cold ($T_e < 10$ eV) and hot plasmas ($T_e > 100$ eV). The DLs associated with bursty bulk flows indicate that the disturbance from magnetic reconnection may have extended nonideal behavior.

The DLs observed inside $\sim 15R_E$ may arise from strong field-aligned currents. Magnetic field lines that are reconnected in the magnetotail are likely to have a moderate degree of tangled topology; the north or south magnetic fields are not connected to their geoconjunctive partner. As the tangled magnetic field lines convect earthward, they require stronger currents to maintain their initial topology. A DL may arise due to these strong currents [11], subsequently changing the magnetic topology. If so, DLs may play an important role in strongly turbulent, collisionless plasmas, for example, astrophysical jets [22,23].

In conclusion, the THEMIS spacecraft have detected double layers in Earth's plasma sheet during enhanced magnetic activity. The DLs are primarily at the plasma sheet boundary layer, near currents ($|\boldsymbol{B}|$ is minimum), and during bursty bulk flows. The occurrence of DLs is such that a significant fraction (1% or more) of the magnetic field lines are undergoing nonideal behavior when active. These observations imply that strongly nonlinear, kinetic behavior is intrinsic to Earth's plasma sheet and, perhaps, to many space and astrophysical plasmas.

This work was supported by NASA grants for THEMIS and FAST, by the German DLR, and by French institutes CNES and CNRS. The authors wish to thank the entire THEMIS team.

[1] H. Alfvén, Space Sci. Rev. **7**, 140 (1967).
[2] L. P. Block, Cosmic Electrodyn. **3**, 349 (1972).
[3] B. H. Quon and A. Y. Wong, Phys. Rev. Lett. **37**, 1393 (1976).
[4] F. S. Mozer *et al.*, Phys. Rev. Lett. **38**, 292 (1977).
[5] R. E. Ergun *et al.*, Phys. Rev. Lett. **87**, 045003 (2001).
[6] L. Andersson *et al.*, Phys. Plasmas **9**, 3600 (2002).
[7] R. E. Ergun *et al.*, Phys. Plasmas **9**, 3685 (2002).
[8] H. Schamel and S. Bujarbarua, Phys. Fluids **26**, 190 (1983).
[9] J. E. Borovsky and G. Joyce, J. Plasma Phys. **29**, 45 (1983).
[10] M. A. Raadu, Phys. Rep. **178**, 25 (1989).
[11] D. L. Newman, M. V. Goldman, R. E. Ergun, and A. Mangeney, Phys. Rev. Lett. **87**, 255001 (2001).
[12] N. Singh, J. Geophys. Res. **108**, 1322 (2003).

[13] D. S. Main, D. L. Newman, and R. E. Ergun, Phys. Rev. Lett. **97**, 185001 (2006).
[14] W. Baumjohann, G. Paschmann, and H. Lühr, J. Geophys. Res. **95**, 3801 (1990).
[15] V. Angelopoulos *et al.*, J. Geophys. Res. **99**, 21 257 (1994).
[16] V. Angelopoulos *et al.*, Space Sci. Rev. **141**, 5 (2008).
[17] J. P. McFadden *et al.*, Space Sci. Rev. **141**, 277 (2008).
[18] J. W. Bonnell *et al.*, Space Sci. Rev. **141**, 303 (2008).
[19] C. M. Cully, R. E. Ergun, K. Stevens, A. Nammari, and J. Westfall, Space Sci. Rev. **141**, 343 (2008).
[20] H. U. Auster *et al.*, Space Sci. Rev. **141**, 235 (2008).
[21] C. T. Russell, Cosmic Electrodyn. **2**, 196 (1971).
[22] J. E. Borovsky, Astrophys. J. **306**, 451 (1986).
[23] M. C. Begelman, R. E. Ergun, and M. J. Rees, Astrophys. J. **625**, 51 (2005).